



## Wound healing in wing membranes of the Egyptian fruit bat (*Rousettus aegyptiacus*) and big brown bat (*Eptesicus fuscus*)

LUCAS J. GREVILLE, ALEJANDRA CEBALLOS-VASQUEZ, ROBERTO VALDIZÓN-RODRÍGUEZ,  
JOHN R. CALDWELL, AND PAUL A. FAURE\*

Department of Psychology, Neuroscience & Behaviour, McMaster University, Hamilton, ON L8S 4K1, Canada

\* Correspondent: [paul4@mcmaster.ca](mailto:paul4@mcmaster.ca)

Bat flight membranes are critical for locomotion, foraging, and physiological homeostasis. Wild bats frequently injure their flight membranes during interactions with the environment and conspecifics or from disease. Researchers biopsy bat wing membranes to mark individuals or collect tissue for taxonomic and molecular studies. Because there are differences in the embryological development of different wing membrane regions, we evaluated differences in flight membrane healing between 2 anatomical regions using 4-mm diameter circular biopsies in the chiroptagium and plagiopatagium of the Egyptian fruit bat (*Rousettus aegyptiacus*; Pteropodiformes) and the insectivorous big brown bat (*Eptesicus fuscus*; Vespertilioniformes). In *R. aegyptiacus*, plagiopatagium wounds took longer to heal to 50% of their initial area compared to chiroptagium wounds; however, this difference was not observed in *E. fuscus*. Plagiopatagium wounds also were more likely to enlarge in the days immediately following biopsy in *R. aegyptiacus* compared to *E. fuscus*. A sigmoid function accurately modeled wound areas and thus healing times in both species. Given the observed differences in wound-healing times between distinct regions of the bat wing membrane, our results indicate that researchers should choose a tissue biopsy location based on the species and question of interest.

Key words: chiroptagium, comparative healing, plagiopatagium, tissue biopsy, flight membranes

Biopsying the flight membranes of bats (Order Chiroptera) was originally proposed as a temporary marking technique (Bonaccorso and Smythe 1972). With the advent of molecular technologies, tissue biopsies have emerged as the most common method for obtaining bat DNA for use in genetic, phylogenetic, and population ecology studies (Wilmer and Barratt 1996; Faure et al. 2009). A typical biopsy involves extending the flight membrane (e.g., wing) against a flat surface and pressing down on the tissue with a sterile biopsy punch tool (Wilmer and Barratt 1996). Although wing punching is not detrimental to flight (e.g., Davis 1968; Weaver et al. 2009), to the best of our knowledge, there are no standard locations for tissue biopsies in bats.

The flight membranes or patagia of bats are divided into 4 sections: the uropatagium or tail membrane, and the wing membranes consisting of the plagiopatagium extending from the dorsum to the fifth digit of the hand, the chiroptagium (also known as the dactylopatagium) extending between the phalanges, and the propatagium extending from the shoulder to the thumb and forming the leading edge of the wing. The skin of the flight membranes is typically mammalian with some

differences in morphology (Gupta 1967; Crowley and Hall 1994). Most mammals have 3 distinct skin layers: the epidermis, dermis, and hypodermis. In the patagia of bats, there is contention over whether the dermis and hypodermis are well defined. There is consensus that the skin forming the wing membrane is composed of an epidermal bilayer (ventral and dorsal) separated by central connective tissue (Murphy 1960; Holbrook and Odland 1978). Within this central region are interstitial structures including sweat and apocrine glands, pilo-sebaceous units, blood and lymphatic vessels, collagen, and elastin fibers (Murphy 1960; Cortese and Nicoll 1970). The tissue composition of the wing also differs between the plagiopatagium, chiroptagium, and uropatagium. In *Myotis ricketti*, the array of cells in the chiroptagium is sparser than in the plagiopatagium (Yin et al. 2011). In *Eptesicus serotinus* and *Nyctalus noctula*, the chiroptagium lacks layers of epidermis, the hypodermis, and skin glands (Kovalyova 2015). The absence of these tissue layers may explain why the chiroptagium also is the thinnest flight membrane, whereas the plagiopatagium is thicker and contains all 3 layers (Crowley and Hall 1994).

Variation in tissue composition of different flight membranes could alter wound-healing times. In the big brown bat (*Eptesicus fuscus*), biopsies from the uropatagium are larger in mass and wounds heal faster than same-sized biopsies in the chiropatagium (Faure et al. 2009; Pollock et al. 2016). Despite this, the chiropatagium remains the most common flight membrane for tissue biopsy (e.g., Sullivan et al. 2006; Bogdanowicz et al. 2012). That said, some studies have started to biopsy the plagiopatagium (e.g., Ellison et al. 2006; Knörnschild et al. 2012).

Increased researcher sampling combined with the tissue lesions that result from infection with the fungus that causes white-nose syndrome has renewed interest in the study of flight membrane wound healing in bats (e.g., Faure et al. 2009; Ceballos-Vasquez et al. 2015; Pollock et al. 2016). The structure of the bat wing makes it highly suitable for experimental work on factors that influence epidermal (cutaneous) healing in the absence of contributions from dermal layers. Moreover, minimal muscle and nervous innervation in the wing, combined with a lack of internal organs, decreases the potential for critical damage or discomfort during biopsy. Bat flight membranes are also relatively easy for researchers to manipulate, alter, and image.

Wound-healing times of the chiropatagium and plagiopatagium have never been compared experimentally. The chiropatagium develops from the persistence of interdigital tissue (Giannini et al. 2006; Adams 2008) caused by inhibition of cell apoptosis (Weatherbee et al. 2006). In contrast, the plagiopatagium forms from overgrowth of the skin adjacent to the proximal regions of the limbs and fifth phalange (Cretkos et al. 2005) and its development relies on the proliferation of tissue from the torso as well as the upper and lower extremities (Kovalyova 2015). We wondered if the developmental changes that give rise to the differing morphologies of the chiropatagium and plagiopatagium during embryogenesis could influence the process of wound healing in adults. To explore this, we conducted a comparative study of wound healing in the chiropatagium and plagiopatagium of 2 bat species from different suborders: the Egyptian fruit bat (*Rousettus aegyptiacus*; Pteropodiformes) from the Yinpterochiroptera, and the big brown bat (*E. fuscus*; Vespertilioniformes) from the Yangochiroptera.

## MATERIALS AND METHODS

**Study animals.**—We tested 24 adult *R. aegyptiacus* (9 female, 15 male) from a captive exhibit housed at the Toronto Zoo, and 17 adult *E. fuscus* (12 female, 5 male) from a captive research colony at McMaster University. Roughly equal numbers of males and females were pseudo-randomly assigned to 1 of 2 groups: 1) tissue biopsy in the left chiropatagium and right plagiopatagium, or 2) tissue biopsy in the right chiropatagium and left plagiopatagium. All females were visually inspected and determined to be nonreproductive at the time of testing.

Animals were kept in husbandry facilities at their respective institutions and were permitted to fly for the duration of the experiment. At McMaster, *E. fuscus* were housed in an indoor, free-flight facility (2.5 × 1.5 × 2.3 m) where the colony temperature and lighting varied with ambient conditions. Bats had ad

libitum access to mealworms (*Tenebrio molitor*), water, and an outdoor flying area (2.5 × 3.8 × 2.7 m—Skrinyer et al. 2017). At the Toronto Zoo, *R. aegyptiacus* were housed in an indoor, free-flight facility (2.9 × 3.1 × 2.6 m) where the colony temperature and lighting (12 h light:dark) were regulated. Bats had ad libitum access to fruit (mainly apples, bananas, grapes, melons, mangoes, kiwis, and pears), water, and a window with ambient light.

**Biopsy procedures.**—Wing biopsies on *R. aegyptiacus* were conducted in January 2014 at the Toronto Zoo under the supervision of a veterinarian. We recorded the mass and forearm length of each bat before anesthetizing it with a 1–5% isoflurane-oxygen gaseous mixture (cone mask, flow rate = 1 l/min). Although anesthesia is typically not used for tissue biopsies of bats in the field, this was a requirement of the Zoo protocol. Anesthetized bats were maneuvered into a supine position and the wing was manually extended in a manner similar to that described by Weaver et al. (2009). We used a circular, sterile Sklar Tru-Punch biopsy tool to excise tissue from a preassigned region of the flight membranes. The chiropatagium and plagiopatagium were biopsied in the same approximate locations in all bats using visual inspection of the phalanges or blood vessels as landmarks. For consistency between individuals, biopsies were conducted by the same experimenter and tissue excisions encompassed the same blood vessel. We used a 4-mm diameter biopsy tool because this punch size is common in bat field studies (e.g., Pollock et al. 2016). The theoretical area ( $A$ ) of a 4-mm diameter (2-mm radius,  $r$ ) circular biopsy is 12.57 mm<sup>2</sup> ( $A = \pi r^2$ ). Tissue biopsies for *E. fuscus* were conducted in August 2014 and followed the same procedures as *R. aegyptiacus*, with the exception that big brown bats were not anesthetized and so they were placed in a custom restrainer immediately prior to tissue biopsy (Ceballos-Vasquez et al. 2014). For consistency, we maintained biopsy landmarks as closely as possible with *R. aegyptiacus* while noting differences in the distribution of blood vessels between species.

All procedures conformed to the guidelines for the care and use of wild mammals in research published by the American Society of Mammalogists (Sikes et al. 2016), care and use of experimental animals published by the Canadian Council on Animal Care, and were approved by the Animal Research Ethics Board of McMaster University.

**Wound measurements.**—We photographed wounds twice per week at alternating 3- and 4-day intervals. The *R. aegyptiacus* photos were taken with a Canon Powershot SD780IS digital camera (Canon, Inc., Melville, New York) attached to a retort stand; the *E. fuscus* photos were collected with a DP25 CCD camera (5 MPixel resolution; Olympus, Tokyo, Japan) mounted to an Olympus SZx10 stereomicroscope (0.63× zoom magnification). In both cases, the wing of the bat was extended to a standard position, using landmarks on a custom restrainer as a guide, so that the membrane laid flat and was directly under and perpendicular to the camera lens. Experimenter judgment was used to ensure that the wing was not over- or underextended. A marker of known dimensions was included in all photos of *R. aegyptiacus* for scaling in case of vertical camera movement on the retort stand. Wound areas (mm<sup>2</sup>) were measured directly

from photographs using ImageJ software (National Institutes of Health—Abramoff et al. 2004) and a calibrated scale (pixels/mm). Image contrast was enhanced prior to automated area calculations to ensure the wound perimeter was visibly distinct from the surrounding tissue.

**Curve fitting.**—Wound area was plotted as a function of days post-biopsy (day 0 = biopsy day), and the data from each bat was fit to a nonlinear least squares sigmoidal function

$$F(x) = ((A - D) / (1 + ((x / C)^B))) + D,$$

where  $x$  is the post-biopsy day number,  $A$  is the maximum asymptote representing the initial wound area on day 0,  $B$  is the healing rate constant representing the steepness of the sigmoid,  $C$  is the inflection point representing the number of days for a wound to reach 50% healed, and  $D$  is the minimum asymptote of 0 representing the area of a fully healed wound. Fitted model parameters were used to compare the healing rate constants (variable  $B$ ) and 50% healing times (variable  $C$ ) between the chiropatagium and plagiopatagium within and between *R. aegyptiacus* and *E. fuscus* (Fig. 1). The inflection point of the modeled curve represents the time required to reach 50% healed, whereas the steepness of the sigmoid reflects the speed of wound closure.

**Statistical analyses.**—Data are reported as the mean  $\pm$  standard deviation ( $\bar{x} \pm SD$ ). Data were first tested for normality and homoscedasticity; non-normal or heteroscedastic data were analyzed with an equivalent nonparametric test. Initial wound areas, healing rate constants, and 50% healing times were compared with independent samples or paired samples statistics, depending if the comparison was between (Welch's  $t$ -test or Mann–Whitney  $U$ -test) or within subjects (paired  $t$ -test or Wilcoxon signed-rank test), respectively. Curve fitting and statistical analyses were performed in Python (SciPy—Python Software Foundation 2017) and R software (R Core Team 2016) using a familywise error rate of  $\alpha = 0.05$ .

Previous observations suggested that the initial wound area frequently increases between day 0 and the next imaging date, typically 2–3 days later (e.g., Church and Warren 1968). We evaluated wound areas of the chiropatagium and plagiopatagium in both species to determine if wound enlargement occurred between days 0–3. Between species, we compared the number of bats with wound enlargement at each biopsy location using a chi-squared test of independence. Within species, the numbers of bats with wound enlargement at each biopsy location were compared with a McNemar chi-squared test of independence.

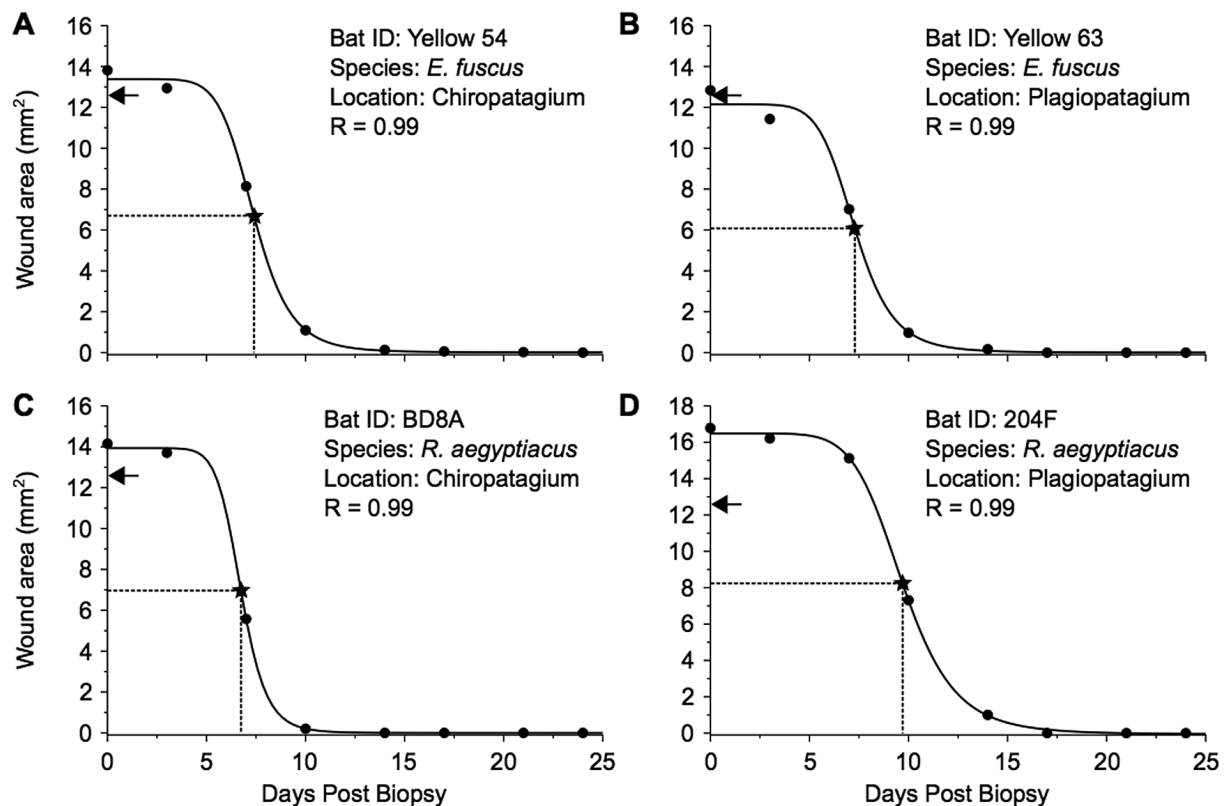


**Fig. 1.**—Measuring wound healing. Each panel shows the fitted sigmoid function and wound area data from the (A) chiropatagium and (B) plagiopatagium of *Eptesicus fuscus*, and from the (C) chiropatagium and (D) plagiopatagium of *Rousettus aegyptiacus*. Two bats are shown for each species. Black circles indicate measured wound areas, and black curves represent fitted 4-parameter sigmoid functions. Note that each function was highly correlated with the raw data ( $R = 0.99$ ,  $P \ll 0.001$  for all curves shown; see equation in text). The estimated (computed) 50% healing time (dotted lines) for each sigmoid is shown as a black star. Black arrows indicate the expected (theoretical) initial wound area ( $12.57 \text{ mm}^2$ ) of a 4-mm diameter circular biopsy. Insets show bat ID#, species, biopsy location, and correlation of sigmoid model fit to raw data.

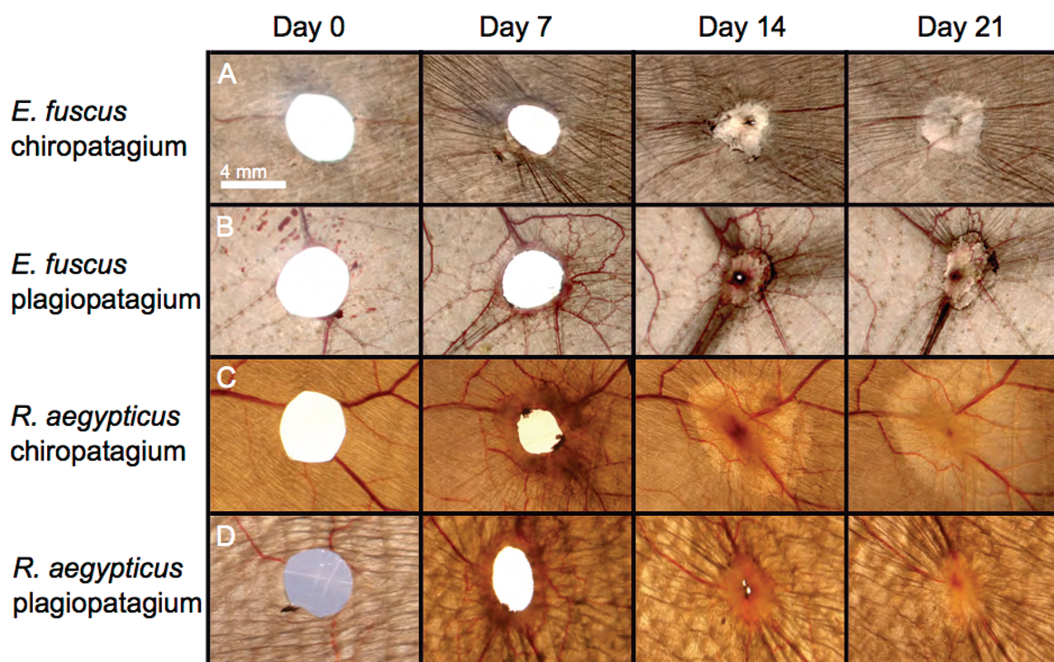


**Fig. 2.**—Images of wing wound healing. Each row shows photographs of the same healing wound on post-biopsy days 0, 7, 14, and 21 in the (A) chiropatagium and (B) plagiopatagium of *Eptesicus fuscus*, and in the (C) chiropatagium and (D) plagiopatagium of *Rousettus aegyptiacus*. Scale bar = 4 mm applies to all panels. Thickening of the wound perimeter and striations caused by tissue contraction around the wound are visible by day 7. Scar tissue undergoing re-pigmentation is evident in newly healed tissue.

## RESULTS

**Study animals.**—All animals maintained good health throughout our experiment as noted by observations of mass, hydration levels, normal behavior, and vocalizations. Bats were weighed each imaging day and visual health checks were completed daily by experimenters or veterinary technicians. The initial masses ( $\bar{x} \pm SD$ ) of female and male *R. aegyptiacus* were  $124.7 \pm 15.7$  g and  $160.3 \pm 16.4$  g, respectively. The initial masses of female and male *E. fuscus* were  $26.5 \pm 4.8$  g and  $21.0 \pm 2.4$  g, respectively.

Between days 0–3, 1 male and 1 female *R. aegyptiacus* tore their chiropatagium from the wound site to the wing margin. Between days 7–10, an additional male *R. aegyptiacus* tore its chiropatagium. It is unclear if these membrane tears occurred during interactions with conspecifics, the captive environment, or from natural movements (e.g., grooming). Upon discovery, the 3 *R. aegyptiacus* with tears were excluded from our study although eventually all of their wings fully healed. We later discovered that the excluded female was pregnant and her gestation occurred without complication. No wing tears were observed in *E. fuscus*.

**Wound-healing times and rate constants.**—We documented wound areas and healing times of 4-mm diameter tissue biopsies in the chiropatagium (Figs. 2A and 2C) and plagiopatagium (Figs. 2B and 2D) of *E. fuscus* (Figs. 2A and 2B) and *R. aegyptiacus* (Figs. 2C and 2D). Once healing began, morphological changes in the chiropatagium and plagiopatagium were quite similar. Thickening of the tissue along the wound perimeter was visible by day 3, with a prominent thickening present by day 7 (Fig. 2). New blood vessel formation was observed as early as day 3 (Fig. 3). Membrane re-pigmentation

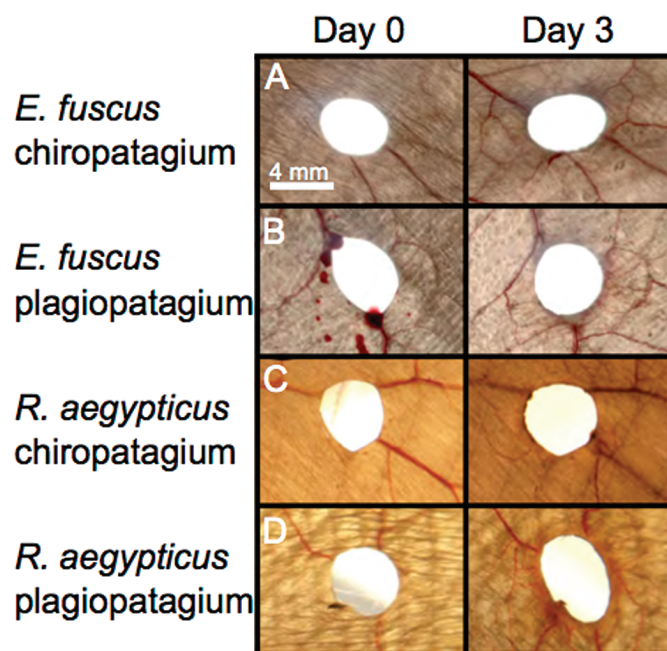


**Fig. 3.**—Wound enlargement in the chiropatagium and plagiopatagium. Rows show examples of wound enlargement (and the corresponding % increase in wound area) between day 0 and post-biopsy day 3 in the (A) chiropatagium (14% increase; Y69) and (B) plagiopatagium (18% increase; Y58) of *Eptesicus fuscus*, and in the (C) chiropatagium (14% increase; 17B2) and (D) plagiopatagium (37% increase; D6B0) of *Rousettus aegyptiacus*. Scale bar = 4 mm applies to all panels.

began to occur by the time wounds were fully healed (Fig. 2, day 14) and continued for months past the end of our experiment (not shown).

We fitted sigmoid functions to the wound area data of the chiropatagium and plagiopatagium of individual *E. fuscus* and *R. aegyptiacus* (Fig. 1). The minimum  $R$ -values for the modeled curves of each species and biopsy condition were: *E. fuscus* chiropatagium,  $R = 0.994$ ; *E. fuscus* plagiopatagium,  $R = 0.988$ ; *R. aegyptiacus* chiropatagium,  $R = 0.995$ ; and *R. aegyptiacus* plagiopatagium,  $R = 0.984$ . Although most wounds followed a similar trend, there was variation in the time and rate of wound healing between individuals within each species and biopsy location (Fig. 4).

Initial wound areas in both species and biopsy locations were almost always larger than the expected (theoretical) area of a 4-mm diameter circle ( $12.57 \text{ mm}^2$ ). Comparing within species, the initial wound areas of the chiropatagium and plagiopatagium of *E. fuscus* were  $13.1 \pm 1.2 \text{ mm}^2$  and  $14.4 \pm 1.7 \text{ mm}^2$ , respectively. For *R. aegyptiacus*, the initial wound areas of the chiropatagium and plagiopatagium were  $14.3 \pm 1.2 \text{ mm}^2$  and  $14.8 \pm 1.3 \text{ mm}^2$ , respectively. Within *E. fuscus*, the initial wound area of the plagiopatagium was larger than that of the chiropatagium ( $t_{16} = -3.47$ ,  $P = 0.003$ ); however, within *R. aegyptiacus* there was no difference in the initial wound areas of the chiropatagium and plagiopatagium ( $t_{20} = 1.24$ ,  $P = 0.23$ ). Comparing between species, the initial wound area of the chiropatagium in *R. aegyptiacus* was larger than in *E. fuscus* (Welch's  $t_{34} = 3.23$ ,  $P = 0.003$ ); however, the initial wound

area of the plagiopatagium did not differ between the species (Welch's  $t_{29} = 0.09$ ,  $P = 0.38$ ).

We used the regressed parameters obtained from the fitted sigmoid functions of each individual to compare the time (number of days for wounds to become 50% healed re: initial area) and rate (healing rate constant) of wound healing for each species and biopsy location (Fig. 5). For *E. fuscus*, there was no difference in the number of days for chiropatagium ( $7.8 \pm 3.0$  days) and plagiopatagium ( $7.5 \pm 2.5$  days) wounds to reach 50% healed (Wilcoxon signed-rank test;  $V = 102$ ,  $P = 0.24$ ). For *R. aegyptiacus*, the 50% healing time of the chiropatagium ( $6.9 \pm 1.0$  days) was shorter than that of the plagiopatagium ( $8.5 \pm 1.5$  days;  $t_{20} = -5.01$ ,  $P = 6.69 \times 10^{-5}$ ).

Between species, there was no difference in the 50% healing time of the chiropatagium between *E. fuscus* ( $7.8 \pm 3.0$  days) and *R. aegyptiacus* ( $6.9 \pm 1.0$  days;  $W = 217$ ,  $P = 0.27$ ), whereas the 50% healing time of the plagiopatagium in *E. fuscus* ( $7.5 \pm 2.5$  days) was slightly shorter compared to that of *R. aegyptiacus* ( $8.5 \pm 1.5$  days;  $W = 96$ ,  $P = 0.01$ ).

We also compared the healing rate constants (sigmoid function variable  $B$ ) between species and biopsy locations. No differences were observed for any of the healing rate constant comparisons (see Table 1).

**Wound enlargement.**—Some wounds increased in size relative to the initial wound area on day 0 in the first 72 h following

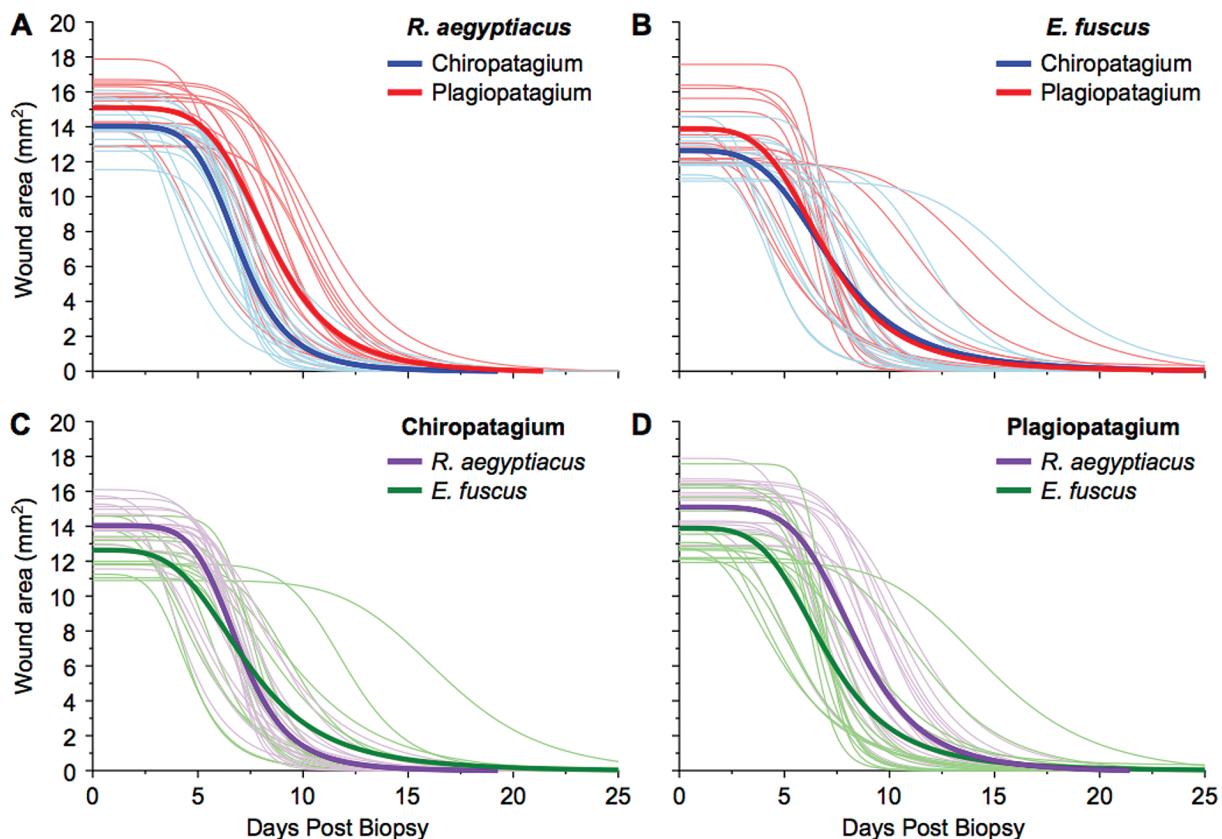


**Fig. 4.**—Modeled wing wound healing. Fitted 4-parameter logistic (sigmoid) functions of wound healing in the chiropatagium and plagiopatagium of *Rousettus aegyptiacus* and *Eptesicus fuscus*. Curves were obtained using a nonlinear, least squares fit to the observed wound area data. Thin lines represent the fitted models for individual bats; thick lines represent the fitted models to the combined data set split by (A and B) membrane biopsy location or (C and D) species.

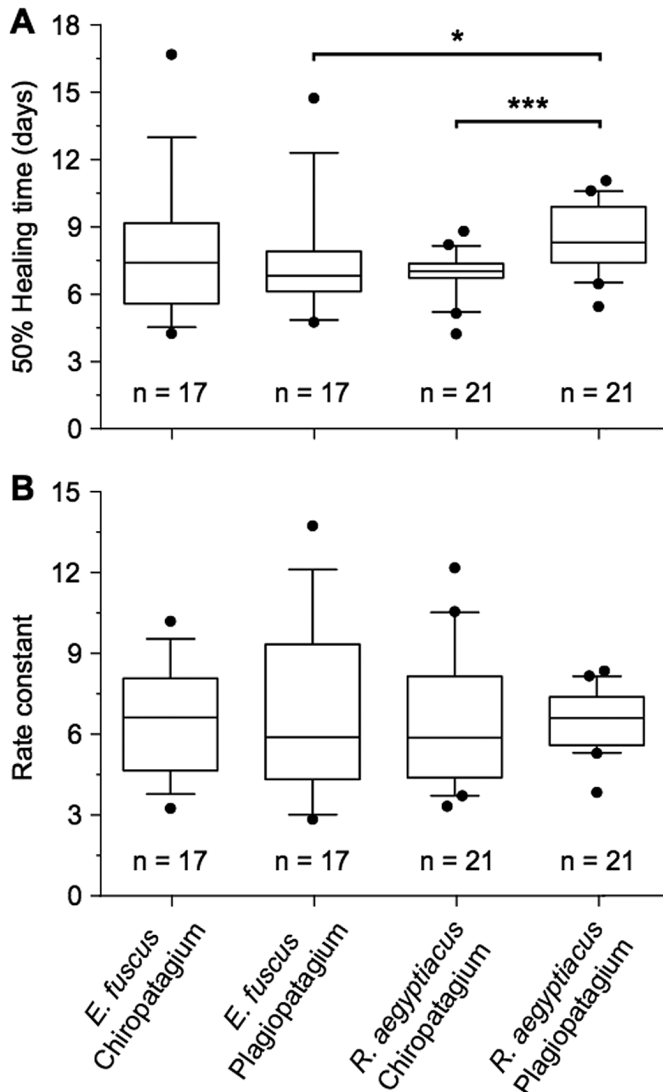


**Fig. 5.**—Time course of wing wound healing. Box plot distributions of (A) 50% healing times and (B) healing rate constants of the chiroptagium and plagiopatagium in *Eptesicus fuscus* and *Rousettus aegyptiacus*. Data were obtained from the values of  $C$  and  $B$ , respectively, of the fitted 4-parameter sigmoid functions for each bat. Boxes extend from the 25th to 75th percentiles, and the solid line within each box is the median value. Error bars above and below the boxes illustrate the 10th and 90th percentiles, with black circles representing individual outlier data points falling outside these values. Significant difference indicated with an asterisk:  $*P < 0.05$ ,  $***P < 0.001$ .

**Table 1.**—Mean  $\pm$  SD healing rate constants derived from fitted modeled curves of wound-healing data in the chiroptagium and plagiopatagium of *Eptesicus fuscus* and *Rousettus aegyptiacus*.

Comparison/healing rate constant ( $\pm$ SD)	Source	Statistical value	P-value
Chiroptagium versus Plagiopatagium			
$6.5 \pm 2.1$ versus $7.1 \pm 3.3$	<i>E. fuscus</i>	$t_{16} = -0.68$	$P = 0.51$
$6.6 \pm 2.5$ versus $5.6 \pm 1.1$	<i>R. aegyptiacus</i>	$t_{20} = 0.10$	$P = 0.92$
<i>E. fuscus</i> versus <i>R. aegyptiacus</i>			
$6.5 \pm 2.1$ versus $6.6 \pm 2.5$	Chiroptagium	Welch's $t_{36} = -0.20$	$P = 0.84$
$7.1 \pm 3.3$ versus $5.6 \pm 1.1$	Plagiopatagium	$W = 180$	$P = 0.10$

membrane biopsy. Wound enlargements occurred in the chiroptagium and plagiopatagium of both species, although they were less frequent in *E. fuscus* compared to *R. aegyptiacus* (Table 2). In *E. fuscus*, 1 chiroptagium (Fig. 3A, ID# Y69) and 1 plagiopatagium (Fig. 3B, ID# Y58), biopsied in different animals, showed wound enlargement of 14% and 18%, respectively. In *R. aegyptiacus*, chiroptagium wound enlargements were observed in 7 bats, plagiopatagium enlargements were observed in 15 bats, and 6 of 7 bats with chiroptagium wound enlargements also had plagiopatagium wound enlargements. In *R. aegyptiacus*, the largest wound enlargements were 14% in the chiroptagium (Fig. 3C, ID# 17B2) and 37% in the plagiopatagium (Fig. 3D, ID# D6B0). Wound enlargements were also more likely in the plagiopatagium of *R. aegyptiacus* than in the plagiopatagium of *E. fuscus*. Within *R. aegyptiacus*, plagiopatagium biopsies had a higher prevalence of wound enlargement than chiroptagium biopsies.

**Summary.**—In *R. aegyptiacus*, the chiroptagium healed faster than the plagiopatagium. In *E. fuscus*, there was no difference in healing time between the chiroptagium and plagiopatagium. The plagiopatagium of *R. aegyptiacus* healed more slowly than the plagiopatagium of *E. fuscus*. Wound enlargement in the 72 h immediately following biopsy occurred more frequently in the plagiopatagium than in the chiroptagium, particularly in *R. aegyptiacus*.

## DISCUSSION

This study compared wound healing in 2 morphologically distinct areas of the bat wing—the chiroptagium and plagiopatagium—in *R. aegyptiacus* and *E. fuscus*. Despite differences in tissue composition between the chiroptagium and plagiopatagium, evolutionary and natural history, animal housing, and diet, wing wound healing in *E. fuscus* and *R. aegyptiacus* followed similar trajectories.

The 50% healing times of the chiroptagium and plagiopatagium in *E. fuscus* did not differ (Fig. 5). This is despite the fact that the initial (starting) wound areas of plagiopatagium biopsies were 9.9% larger than chiroptagium biopsies (Figs. 4A and 4B). The difference in initial wound areas could have resulted from differential wound contraction immediately following biopsy. Wound contraction occurs when elastin fibers in the membrane contract following biopsy (Gosline et al. 2002). A detailed analysis of tissue composition is needed to determine if the composition of elastin fibers in the chiroptagium differs

**Table 2.**—Total number and relative frequency of wound enlargement in the chiropatagium and plagiopatagium of *Eptesicus fuscus* and *Rousettus aegyptiacus*.

Comparison/frequency ( <i>n</i> )		Source	Statistical value	<i>P</i> -value	
Chiropatagium	versus	Plagiopatagium			
8		16	Species combined	$X^2_1 = 2.98$	$P = 0.084$
1/17		1/17	<i>E. fuscus</i>	McNemar $X^2_1 = 0$	$P = 1$
7/21		15/21	<i>R. aegyptiacus</i>	McNemar $X^2_1 = 4.90$	$P = 0.027$
<i>E. fuscus</i>	versus	<i>R. aegyptiacus</i>			
2		22	Locations combined	$X^2_1 = 16.71$	$P = 4.35e-05$
1/17		7/21	Chiropatagium	$X^2_1 = 2.77$	$P = 0.096$
1/17		15/21	Plagiopatagium	$X^2_1 = 13.98$	$P = 1.85e-04$

from that of the plagiopatagium. Despite the unintended difference in starting wound areas, the plagiopatagium of *E. fuscus* managed to heal as quickly as the chiropatagium. This finding also suggests that the plagiopatagium may actually heal faster than the chiropatagium. Additional experiments are needed to test this hypothesis.

Our data align with previous studies in bats reporting initial wound areas larger than expected (theoretical) wound areas (Fig. 4; Davis and Doster 1972; Faure et al. 2009; Pollock et al. 2016), and an increase in wound size (i.e., wound enlargement) in the days immediately following biopsy (Fig. 3; Church and Warren 1968; Faure et al. 2009; Pollock et al. 2016). In this study, we examined the frequency of wound enlargement on post-biopsy day 3 and found that enlarged wounds were more common in *R. aegyptiacus* than *E. fuscus*, and that wound enlargement was more likely to occur in the plagiopatagium.

Slower healing times were observed for the plagiopatagium of *R. aegyptiacus*. These results may be species-specific and influenced by a higher prevalence of collagen and elastin within the plagiopatagium of *R. aegyptiacus*. Collagen and elastin fibers become damaged during biopsy and, owing to their tensile properties, this can result in wound enlargement (Gosline et al. 2002). If true, then differences in the quantity and distribution of collagen and elastin fibers in the chiropatagium and plagiopatagium are expected to correlate with the different frequencies of wound enlargement in *E. fuscus* and *R. aegyptiacus*. Other non-mutually exclusive explanations for wound enlargements include interactions with conspecifics or the environment, and overextension of the wing by the experimenter during wound imaging, which also would cause collagen and elastin fibers to become overstretched (Holbrook and Odland 1978). A greater prevalence of wound enlargement in *R. aegyptiacus* may account for the observed increase in 50% healing time of the plagiopatagium compared to the chiropatagium (Figs. 2 and 5).

It remains difficult to make cross-study comparisons of flight membrane healing times in bats owing to differences in species, housing conditions, biopsy sizes, and biopsy locations. In captivity, wing membrane healing has been studied in straw-colored fruit bats (*Eidolon helvum*—Church and Warren 1968), pallid bats (*Antrozous pallidus*—Davis and Doster 1972), and big brown bats (Faure et al. 2009; Ceballos-Vasquez et al. 2015). In the field, healing has been documented for Bechstein's bats (*Myotis bechsteinii*—Kerth et al. 2002), little

brown bats (*Myotis lucifigus*—Weaver et al. 2009), big brown bats (Pollock et al. 2016), and African vespertilionids (*Hypsugo anchietae*, *Neoromicia zuluensis*, and *Pipistrellus rusticus*—Pierce and Keith 2011). Fuller et al. (2011) documented healing in the wings of *M. lucifigus* following lesion damage caused by the psychrophilic fungus (*Pseudogymnoascus destructans*) that is associated with white-nose syndrome in bats. Despite this variation, together with our data these studies demonstrate the remarkable capability of the bat wing to quickly and fully heal.

Researchers do not yet understand how wing damage impedes locomotion and foraging in bats. We know bats can sustain flight despite large holes in their flight membranes (Davis 1968). Flight membrane damage is thought to negatively impact wing physiology and foraging success (Reichard and Kunz 2009). Consistent with this notion, bats with wing defects perform fewer U-turns in mid-flight (Voigt 2013). Moreover, negative effects of flight membrane damage may be exacerbated in wild, free-ranging bats compared to bats in captivity. Although environmental sources of membrane damage are present in both situations, aerial foraging is greatly reduced in captive bats. Pollock et al. (2016) observed longer healing times in wild *E. fuscus* compared to healing of same-sized wounds for *E. fuscus* in captivity (Faure et al. 2009). This suggests that negative effects associated with flight membrane damage, such as reduced foraging success, may be exacerbated in wild animals and occur over an extended period.

Our study clearly demonstrates the power of mathematical models to generate fitted functions that can accurately estimate critical parameters of wound healing (Cukjati et al. 2001). Models make it relatively easy to calculate and standardize arbitrary healing milestones (e.g., the time required to reach 10%, 25%, 50%, 75%, or 90% wound closure). Because most healing studies, including our own, image wounds at predetermined sampling intervals, they risk missing important milestones due to the temporal resolution of their imaging protocol. This risk can be mitigated by increasing the frequency of wound imaging; however, this increases the frequency of animal handling, which can exacerbate wounds and alter the healing process. For example, mechanical deformation (i.e., overstretching) of tissues by experimenter handling has been suggested to impede healing in some studies (Holbrook and Odland 1978), yet others suggest that it can facilitate healing via myofibroblast formation (Squier 1981). Distress due to handling and restraint could alter wound-healing times due

**Table 3.**—Mean  $\pm$  SD number of post-biopsy days to reach 10%, 25%, 50%, 75%, and 90% wound closure in the chiropatagium or plagiopatagium of *Eptesicus fuscus* ( $n = 17$ ) and *Rousettus aegyptiacus* ( $n = 21$ ). For comparison, also shown are sigmoid curve model estimates for the fitted data from each individual.

Species	Biopsy location	% closure	Measured		Modeled	
			Mean	SD	Mean	SD
<i>E. fuscus</i>	Chiropatagium	10	5.5	3.0	5.5	2.4
		25	8.2	2.9	6.6	2.7
		50	9.4	2.8	7.8	3.0
		75	11.1	3.5	9.3	3.4
		90	12.4	4.1	11.2	3.9
	Plagiopatagium	10	5.1	2.1	5.2	1.9
		25	7.6	1.8	6.2	2.1
		50	8.9	2.9	7.5	2.5
		75	11.1	2.9	9.0	2.9
		90	11.9	3.4	10.8	3.5
<i>R. aegyptiacus</i>	Chiropatagium	10	6.0	1.7	4.8	1.1
		25	7.1	0.7	5.7	1.1
		50	8.4	1.5	6.9	1.0
		75	10.2	1.4	8.2	1.1
		90	11.7	2.0	9.9	1.4
	Plagiopatagium	10	7.5	2.0	6.1	1.3
		25	8.7	1.5	7.2	1.4
		50	10.5	2.2	8.5	1.5
		75	12.3	2.0	10.0	1.7
		90	13.7	1.8	11.9	1.8

to changes in hormone levels or immune function (Guo and Dipietro 2010; Archie 2013). Our sigmoid models strongly fit the observed experimental healing data (Figs. 1 and 4). This means that researchers can use models to accurately estimate specific sampling times to collect raw imaging data that capture histological changes of interest or critical milestones of healing and reduce the frequency of experimenter handling of animals (Table 3).

In addition to supporting the use of quantitative modeling in wound healing research, we hope our study will help inform investigators about the most suitable locations for tissue biopsy in field studies with bats. For example, in phylogenetic and molecular studies, researchers should collect tissue biopsies from faster-healing membranes, whereas in mark-and-recapture studies, researchers should biopsy slower-healing membranes to facilitate the short-term identification of previously captured animals that were otherwise unmarked.

#### ACKNOWLEDGMENTS

At the Toronto Zoo, we thank senior veterinarian Dr. G. Crawshaw for assistance with protocol development, animal anesthesia, and tissue biopsies, zookeeper C. Guthrie for care and maintenance of the *R. aegyptiacus* colony, and curator of mammals M. Franke for support and access to animals and the facility. At McMaster University, we thank university veterinarian Dr. K. Delaney for assistance with animal health and protocol development, and technician D. Graham for care and maintenance of the *E. fuscus* colony. H. Zhang assisted with wound imaging. Research

supported by a Discovery Grant from the Natural Sciences and Engineering Research Council of Canada, and infrastructure grants from the Canada Foundation for Innovation and the Ontario Innovation Trust (PAF).

#### LITERATURE CITED

- ABRAMOFF, M. D., P. J. MAGALHAES, AND S. J. RAM. 2004. Image processing with ImageJ. *Biophotonics International* 11:36–42.
- ADAMS, R. A. 2008. Morphogenesis in bat wings: linking development, evolution and ecology. *Cells, Tissues, Organs* 187:13–23.
- ARCHIE, E. A. 2013. Wound healing in the wild: stress, sociality and energetic costs affect wound healing in natural populations. *Parasite Immunology* 35:374–385.
- BOGDANOWICZ, W., K. PIKSA, AND A. TEREBA. 2012. Genetic structure in three species of whiskered bats (genus *Myotis*) during swarming. *Journal of Mammalogy* 93:799–807.
- BONACCORSO, F., AND N. SMYTHE. 1972. Punch-marking bats: an alternative to banding. *Journal of Mammalogy* 53:389–390.
- CEBALLOS-VASQUEZ, A., J. R. CALDWELL, AND P. A. FAURE. 2014. A device for restraining bats. *Acta Chiropterologica* 16:255–260.
- CEBALLOS-VASQUEZ, A., J. R. CALDWELL, AND P. A. FAURE. 2015. Seasonal and reproductive effects on wound healing in the flight membranes of captive big brown bats. *Biology Open* 4:95–103.
- CHURCH, J. C., AND D. J. WARREN. 1968. Wound healing in the web membrane of the fruit bat. *The British Journal of Surgery* 55:26–31.
- CORTESE, T. A., JR., AND P. A. NICOLL. 1970. *In vivo* observations of skin appendages in the bat wing. *The Journal of Investigative Dermatology* 54:1–10.
- CRETEKOS, C. J., ET AL. 2005. Embryonic staging system for the short-tailed fruit bat, *Carollia perspicillata*, a model organism for the mammalian order Chiroptera, based upon timed pregnancies in captive-bred animals. *Developmental Dynamics* 233:21–738.
- CROWLEY, G. V., AND L. S. HALL. 1994. Histological observations on the wing of the grey-headed flying-fox (*Pteropus poliocephalus*) (Chiroptera, Pteropodidae). *Australian Journal of Zoology* 42:215–231.
- CUKJATI, D., S. REBERSEK, AND D. MIKLAVCIC. 2001. A reliable method of determining wound healing rate. *Medical & Biological Engineering & Computing* 39:263–271.
- DAVIS, R. 1968. Wing defects in a population of pallid bats. *American Midland Naturalist* 79:388–395.
- DAVIS, R., AND S. E. DOSTER. 1972. Wing repair in pallid bats. *Journal of Mammalogy* 53:377–378.
- ELLISON, L. E., ET AL. 2006. Sampling blood from big brown bats (*Eptesicus fuscus*) in the field with and without anesthesia: impacts on survival. *Journal of Wildlife Diseases* 42:849–852.
- FAURE, P. A., D. E. RE, AND E. L. CLARE. 2009. Wound healing in the flight membranes of big brown bats. *Journal of Mammalogy* 90:1148–1156.
- FULLER, N. W., J. D. REICHARD, M. L. NABHAN, S. R. FELLOWS, L. C. PEPIN, AND T. H. KUNZ. 2011. Free-ranging little brown myotis (*Myotis lucifugus*) heal from wing damage associated with white-nose syndrome. *EcoHealth* 8:154–162.
- GIANNINI, N., A. GOSWAMI, AND M. R. SÁNCHEZ-VILLAGRA. 2006. Development of integumentary structures in *Rousettus amplexicaudatus* (Mammalia: Chiroptera: Pteropodidae) during late-embryonic and fetal stages. *Journal of Mammalogy* 87:993–1001.
- GOSLINE, J., M. LILLIE, E. CARRINGTON, P. GUERETTE, C. ORTLEPP, AND K. SAVAGE. 2002. Elastic proteins: biological roles and mechanical properties. *Philosophical Transactions of the Royal Society of London, B. Biological Sciences* 357:121–132.

- GUO, S., AND L. A. DIPIETRO. 2010. Factors affecting wound healing. *Journal of Dental Research* 89:219–229.
- GUPTA, B. B. 1967. The histology and musculature of plagiopatagium in bats. *Mammalia* 31:313–321.
- HOLBROOK, K. A., AND G. F. ODLAND. 1978. A collagen and elastic network in the wing of the bat. *Journal of Anatomy* 126:21–36.
- KERTH, G., F. MAYER, AND E. PETIT. 2002. Extreme sex-biased dispersal in the communally breeding, nonmigratory Bechstein's bat (*Myotis bechsteinii*). *Molecular Ecology* 11:1491–1498.
- KNÖRNSCHILD, M., M. NAGY, M. METZ, F. MAYER, AND O. VON HELVERSEN. 2012. Learned vocal group signatures in the polygynous bat *Saccopteryx bilineata*. *Animal Behaviour* 84:761–769.
- KOVALYOVA, I. M. 2015. Comparative aspects of the morphogenesis and morphology of the wing membranes of bats (Chiroptera) and flying lemurs (Dermoptera). *Vestnik Zoologii* 49:451–456.
- MURPHY, R. C. 1960. Fluorescence studies in the wing of the living bat. *The Anatomical Record* 136:127–135.
- PIERCE, M. W., AND M. KEITH. 2011. Healing rates of wing membranes in two species of Vespertilionid bats. *African Bat Conservation News* 25:3–5.
- POLLOCK, T., C. R. MORENO, L. SÁNCHEZ, A. CEBALLOS-VASQUEZ, P. A. FAURE, AND E. C. MORA. 2016. Wound healing in the flight membranes of wild big brown bats. *The Journal of Wildlife Management* 80:19–26.
- PYTHON SOFTWARE FOUNDATION. 2017. Python language reference, version 2.7. <http://www.python.org>. Accessed 10 January 2014.
- R CORE TEAM. 2016. R: a language and environment for statistical computing. R Foundation for Statistical Computing, Vienna, Austria.
- REICHARD, J. D., AND T. H. KUNZ. 2009. White-nose syndrome inflicts lasting injuries to the wings of little brown myotis (*Myotis lucifugus*). *Acta Chiropterologica* 11:457–464.
- SIKES, R. S., AND THE ANIMAL CARE AND USE COMMITTEE OF THE AMERICAN SOCIETY OF MAMMALOGISTS. 2016. 2016 Guidelines of the American Society of Mammalogists for the use of wild mammals in research and education. *Journal of Mammalogy* 97:663–688.
- SKRINYER, A. J., ET AL. 2017. Care and husbandry of the world's only flying mammals. *Laboratory Animal Science Professional* June:24–27.
- SQUIER, C. A. 1981. The effect of stretching on formation of myofibroblasts in mouse skin. *Cell and Tissue Research* 220:325–335.
- SULLIVAN, J., K. BUSCETTA, AND R. MICHENER. 2006. Models developed from  $\delta^{13}\text{C}$  and  $\delta^{15}\text{N}$  of skin tissue indicate non-specific habitat use by the big brown bat (*Eptesicus fuscus*). *Ecoscience* 13:11–22.
- VOIGT, C. C. 2013. Bat flight with bad wings: is flight metabolism affected by damaged wings? *Journal of Experimental Biology* 216:1516–1521.
- WEATHERBEE, S. D., R. R. BEHRINGER, J. J. RASWEILER, AND L. A. NISWANDER. 2006. Interdigital webbing retention in bat wings illustrates genetic changes underlying amniote limb diversification. *Proceedings of the National Academy of Sciences* 103:15103–15107.
- WEAVER, K. N., S. E. ALFANO, A. R. KRONQUIST, AND D. M. REEDER. 2009. Healing rates of wing punch wounds in free-ranging little brown Myotis (*Myotis lucifugus*). *Acta Chiropterologica* 11:220–223.
- WILMER, J. W., AND E. BARRATT. 1996. A non-lethal method of tissue sampling for genetic studies of chiropterans. *Bat Research News* 37:1–3.
- YIN, J. X., H. M. WANG, P. RACEY, AND S. Y. ZHANG. 2011. Microanatomy of the fishing bat skin. *Pakistan Journal of Zoology* 43:387–392.

Submitted 22 November 2017. Accepted 30 April 2018.

Associate Editor was Jorge Ortega.